JOURNAL OF ENDOUROLOGY
Volume 33, Number 2, February 2019

Pp. 113–119
DOI: 10.1089/end.2018.0485

Simulation of Laser Lithotripsy-Induced Heating in the Urinary Tract

Adam D. Maxwell, PhD,[1,2] Brian MacConaghy, MS,[2] Jonathan D. Harper, MD,[1] Ali H. Aldoukhi, MD,[3] Timothy L. Hall, PhD,[4] and William W. Roberts, MD[3,4]

Abstract

Purpose: Holmium laser lithotripsy is a common modality used to fragment urinary stones during ureteroscopy. Laser energy deposited during activation produces heat and potentially causes thermal bioeffects. We aimed to characterize laser-induced heating through a computational simulation.

Materials and Methods: A finite-element model was developed and used to estimate temperature in the urinary tract. Axisymmetric models of laser lithotripsy in a renal calyx, the renal pelvis, and proximal ureter were created. Heat generation by laser and heat transfer were simulated under different laser powers between 5 and 40 W. Irrigation fluid flow was introduced at rates between 0 and 40 mL/min. The model was validated by comparison with previous *in vitro* temperature data in a test tube, then used to calculate heating and thermal dose in the three tissue models.

Results: Simulated temperature rises agreed well with most *in vitro* experimental measurements. In tissue models, temperature rises depended strongly on laser power and irrigation rate, and to a lesser extent on location. Injurious temperatures were reached for 5–40 W laser power without irrigation, >10 W with 5 mL/min irrigation, 40 W with 15 mL/min irrigation, and were not found at 40 mL/min irrigation. Tissue injury volumes up to 2.3 cm^3 were calculated from thermal dose.

Conclusions: The results suggest a numerical model can accurately simulate the thermal profile of laser lithotripsy. Laser heating is strongly dependent on parameters and may cause a substantial temperature rise in the fluid in the urinary tract and surrounding tissue under clinically relevant conditions.

Keywords: laser lithotripsy, urinary stone, ureteroscopy

Introduction

Urinary tract stones are commonly treated by three procedures: shockwave lithotripsy (SWL), ureteroscopy (URS), and percutaneous nephrolithotomy. SWL and URS are used in >90% of cases.[1] Although SWL is at present the only truly noninvasive intervention, its use has been declining in favor of URS,[1] which has become more effective with improvements to the technology.[2] SWL has not seen such advances in efficacy, although several emerging technologies may eventually improve it.[3–5]

URS for stone treatment is performed almost exclusively using laser lithotripsy, where a fiber-optic Holmium:YAG laser generates pulses with sufficient energy to produce stone disintegration.[6] This instrument operates in different modes to produce either fragments to be removed through basket, or dust that will expel spontaneously from the urinary tract.

In recent years, laser parameters with higher power have been advocated to increase efficiency. However, most of the energy deposited by the laser ultimately converts to heat. *In vitro* and *in vivo* studies have suggested that laser lithotripsy may produce substantial heat during procedures through repeated laser pulsing.[7–11] In conjunction with fluid irrigation, it is not clear how heat dissipation evolves during URS.

We propose that the thermal profile of laser lithotripsy can be evaluated through computational simulations in conjunction with physical experiments. Such models can complement experimental data and allow systematic investigation of clinical and biological factors affecting heating. In this study, we first compare our simulation with *in vitro* experiments[7] to validate its accuracy. We then simulate several cases of laser lithotripsy to evaluate the fluid and tissue temperature distribution and parameters controlling heating.

[1]Department of Urology, University of Washington School of Medicine, Seattle, Washington.
[2]Applied Physics Laboratory, University of Washington, Seattle, Washington.
[3]Department of Urology, University of Michigan, Ann Arbor, Michigan.
[4]Department of Biomedical Engineering, University of Michigan, Ann Arbor, Michigan.

Materials and Methods

Experiment

The experimental setup and tests are fully described in a separate article.[7] In brief, the setup consisted of a water tank filled with 14 L of 37°C deionized water, with a submerged 10 mm diameter glass test tube simulating a human calyx and positioned with the opening 1 cm above the bath surface. A lithotripsy laser system (pulse 120; Lumenis, San Jose, CA) was used with the laser fiber passed through the working channel of an ureteroscope. The fiber was positioned 15 mm from the bottom of the tube and the ureteroscope was held 20 mm from the bottom. A thermocouple was held 5 mm from the bottom ~2 mm lateral from the position of the laser to record temperature.

Room temperature irrigation was introduced for 20 seconds before laser activation. Different laser parameters were used in each trial, with pulse energies and pulse repetition frequencies of 0.5 J × 10 Hz (5 W), 1.0 J × 10 Hz or 0.5 J × 20 Hz (10 W), 1.0 J × 20 Hz or 0.5 J × 40 Hz (20 W), 1.0 J × 40 Hz or 0.5 J × 80 Hz (40 W), and irrigation flow of 0, 15, or 40 mL/min for 60 seconds. The laser was then deactivated and irrigation was continued for 20 seconds.

Numerical simulation

Numerical simulations were performed on a workstation computer in COMSOL Multiphysics finite-element modeling software (COMSOL, Burlington, MA). The numerical model included heat transfer components of diffusion, convection, and sourcing. Fluid was modeled to include laminar flow, and heat-induced convection and mixing. An axisymmetric model was used to minimize calculation time.

The experimental setup from the previous section was first simulated for model validation. The test tube was surrounded by water, approximating the large water bath in experiments. The tube was 10 mm diameter and 55 mm length (volume 8.1 mL) with 1 mm wall thickness (Fig. 1), with an open continuous flow boundary condition (fluid flows out of the tube during irrigation). The laser was modeled as a 0.5 mm diameter heat source in the center of the test tube 15 mm above the bottom surface. Laser radiation force was modeled as a volume force in the fluid. A 1 mm diameter tube was positioned 5 mm above the laser source as an irrigation inlet. Irrigation was introduced at 22°C with rates between 0 and 40 mL/min. Fluid velocities and temperature were calculated for all spatial points in the model. The average temperature within the entire test tube volume was also calculated.

For simulations of *in vivo* cases, we modeled three simplified scenarios in the proximal ureter, the renal pelvis, and a renal calyx. All material parameters are included in Table 1. Most physical dimensions applied here are approximated from literature measurements captured by urography, CT, or MRI,[12–14] although these vary substantially between individuals. Cooling effects from blood perfusion were modeled in the tissues. The three models were axisymmetric to reduce computational complexity (Fig. 1).

(1) The calyx was modeled as a 6 mm diameter by 5 cm length tube (volume 2.7 mL) with 1 mm collecting system wall that terminated 15 mm from the laser similar to the geometry of the test tube. The wall was surrounded by kidney parenchyma.
(2) The renal pelvis was modeled as a 2 cm diameter spherical fluid-filled chamber with 6 mm diameter tube extending for 7.5 cm from one side to simulate the ureter (volume 8.7 mL). The urinary tract was lined with a 1 mm wall. The laser and irrigation were positioned at the orifice between the ureter and pelvis. Kidney tissue surrounded the collecting system and ureter wall.
(3) The ureter model was simulated in the same geometric model as the renal pelvis, but the laser was placed 4.5 cm from the opening of the collecting space and the irrigation placed 5 mm distal to the laser.

The thermal dose was calculated to estimate the extent of tissue damage. Thermal dose is a common metric based on empirical data that combines temperature and exposure time of a tissue to estimate when tissue is considered nonviable:

$$TD_{43} = \int_0^\infty R^{43-T} dt. \quad (1)$$

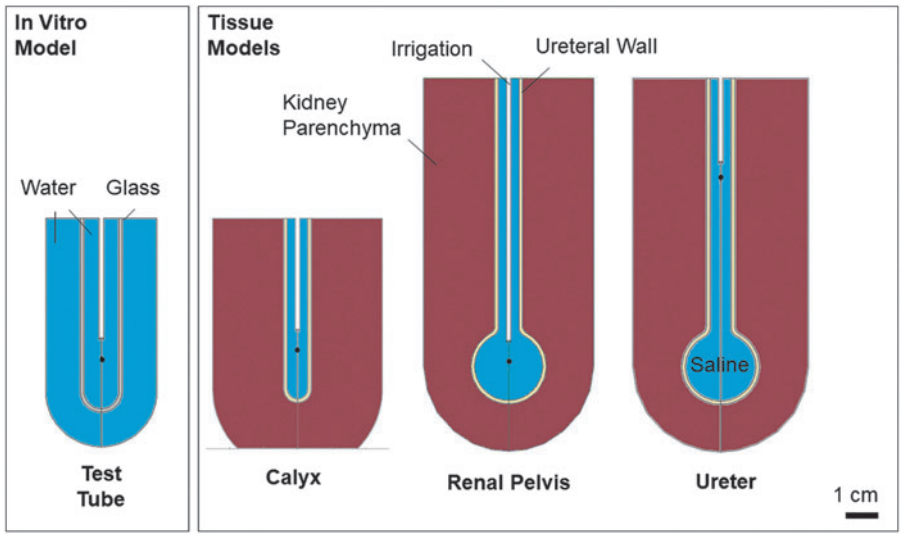

FIG. 1. Model geometry for the *in vitro* test tube simulations (*left*), as well as the calyx (*center left*), renal pelvis (*center right*), and ureter (*right*) simulations. An irrigation tube is inserted at the center axis of each model, with the heat source represented below it as a *black circle*. Material areas are separated by color.

TABLE 1. MATERIAL AND TISSUE PARAMETERS USED FOR SIMULATIONS OF *IN VITRO* AND *IN VIVO* CONDITIONS

	Density (kg/m^3)	*Specific heat capacity (J/kg·K)*	*Thermal conductivity (W/m·K)*	*Perfusion rate (L/min·kg)*
Water	998	4184	0.608	—
Glass	2230	750	0.800	—
Urine	1023	4178	0.560	—
Blood	1049	3617	0.517	—
Urinary tract wall	1101	3306	0.462	0.19
Kidney parenchyma	1049	3587	0.527	3.80

In Equation 1, T is temperature, t is time, R is a factor (0.25 for $T<43$°C and 0.5 for $T\geq 43$°C), and TD_{43} is the thermal dose, in cumulative equivalent minutes held at 43°C. Tissue is considered denatured for $TD_{43}>240$ minutes.[15,16] Thermal dose is a strongly nonlinear function of temperature; it takes 240 minutes to render tissue nonviable at 43°C, but only ~15 seconds at 53°C.

Laser powers (calculated from pulse energy and rate) between 5 and 40 W were considered at irrigation rates of 0, 5, 15, and 40 mL/min in each model.

Results

In vitro *simulation and validation*

Without irrigation, heat accumulated around the laser and radiated in a nearly symmetric manner, with temperature increasing until termination of laser pulsing. With irrigation, heat was carried with the fluid toward the distal surface of the test tube, which impacted and then displaced toward the tube opening, causing mixing of the fluid and a more uniform temperature throughout the tube. Heat dissipated after laser cessation.

Quantitatively, thermocouple temperature (10 mm distal and 2 mm lateral from laser fiber) reached >100°C at 0 mL/min irrigation in simulation, whereas the volume-averaged temperature in the tube reached up to 68°C at the highest laser power of 40 W in both experiment and simulation (Table 2). Peak temperatures in experiments were nearly identical with parameters of the same power regardless of pulse setting or frequency. Temperatures >100°C are unlikely in the fluid for even a short duration because of boiling that is not captured in these simulations. Instead, the volume-averaged temperature in the test tube gave more reasonable estimates of temperature rise expected in well-mixed fluid. Without irrigation, a significant discrepancy exists between experimental measurements and those in simulation, particularly in cases where boiling is predicted. Simulations and experiments without irrigation agree well provided fluid mixing is introduced (Fig. 2). This is demonstrated by simulations where we artificially increased the radiation force of the laser on the fluid, causing enhanced mixing. This change does not cause a significant difference with irrigation that causes mixing naturally.

With 15 and 40 mL/min irrigation, temperature rises were reduced. However, temperatures >43°C occurred with 15 mL/min irrigation at 40 W laser power. At 40 mL/min of irrigation, temperature never reached >37°C under any condition. Temperature elevation in simulations compared favorably with experiments, with a maximum difference of 6°C rise (Fig. 2 and Table 2).

TABLE 2. MAXIMUM TEMPERATURES REACHED IN EXPERIMENT AND SIMULATION

Irrigation (mL/min)	*Power (W)*	*Experiment TC (°C)*	*Simulation TC (°C)*	*Simulation average (°C)*
0	5	47	85	46
	10	52	104	50
	20	56	100	57
	40	68	244	68
15	5	30	28	28
	10	34	32	32
	20	42	42	40
	40	50	60	56
40	20	30	30	30
	40	37	37	37

TC = thermocouple temperature.

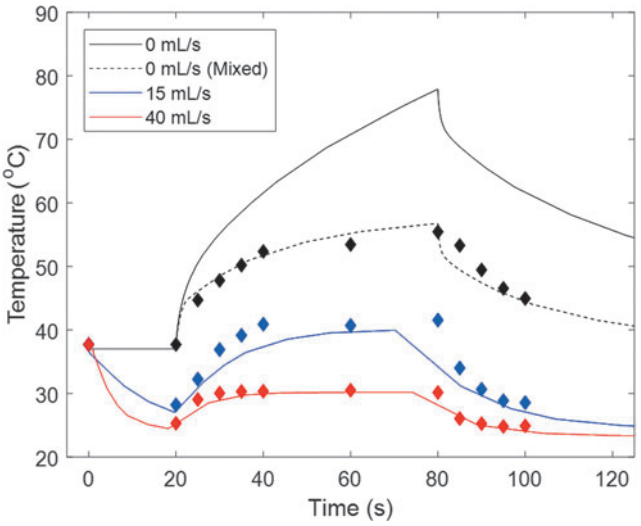

FIG. 2. Temporal thermal profiles measured by thermocouple (*points*) and simulated volume-averaged fluid temperature (*lines*) in the test tube for 20 W laser power at different irrigation rates. Curves follow an initial steep rise with initiation of laser firing at 20 seconds, but approach an asymptotic value, particularly at 15 and 40 mL/min irrigation levels. The simulation overpredicts temperature rise for no irrigation because of absence of fluid mixing the simulation. Artificially forcing this mixing produces better agreement (*dashed line*).

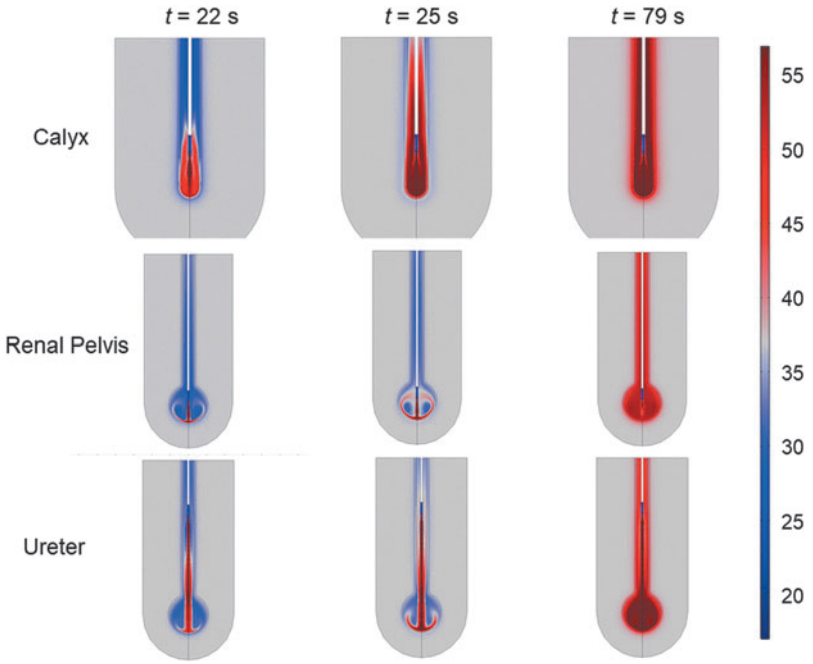

FIG. 3. Example images of heat deposition in the calyx (*top row*), renal pelvis (*center row*), and ureter (*bottom row*) models at three time points with laser power of 40 W and irrigation rate of 15 mL/min. The *color bar* indicates temperature (°C).

Simulation of heating in caliceal fluid and tissue

Simulations of heating in the urinary tract showed similar trends to those *in vitro*. Without irrigation, heat deposited around the laser fiber, causing tissue to receive thermal doses sufficient to cause irreversible damage. With irrigation, heat was distributed over larger regions. In all three locations, irrigation carried the heat retrograde and impinged on the distal surface of the collecting system before deflecting anterograde, after which the fluid temperature reached a more uniform value by mixing. Significant temperature rises and injury could occur far from the fiber (Fig. 3). For instance, with high irrigation and laser power, heat deposited in the ureter caused injury at the distal surface of the renal pelvis 6.5 cm away from the laser. In severe cases, injury was predicted in both the collecting system wall and the kidney parenchyma.

Without irrigation, volume-averaged fluid temperatures of 44°C to >100°C were achieved (Fig. 4). Temperatures in the calyx were greater than the other two locations for the same laser power. Irrigation at 5 mL/min resulted in fluid temperatures between 36.5°C and 99.6°C, depending on the power and location. Peak tissue temperatures were ≥46°C, sufficient to cause thermal bioeffects for ≥10 W laser power. Peak temperatures for 15 and 40 mL/min irrigation ranged from 37.2°C to 79°C and 37.0°C to 40.5°C, respectively. Thus, irrigation could almost entirely mitigate heating.

Injury volumes calculated based on a thermal dose for 43°C > 240 minutes varied strongly with laser power and irrigation rate, and less so with location. Injury occurred for the following conditions regardless of location: ≥5 W power at 0 mL/min irrigation, ≥10 W power at 5 mL/min, and 40 W power at 15 mL/min. No thermal injury was produced at 40 mL/min. Injury to the parenchyma was generated only with irrigation ≤5 mL/min. Injury volumes up to 2.35 cm^3 occurred (Fig. 5). The laser activation time required to initiate injury reduced with increasing laser power. The time to initial injury with irrigation was <1–21 seconds (Fig. 6). Certain

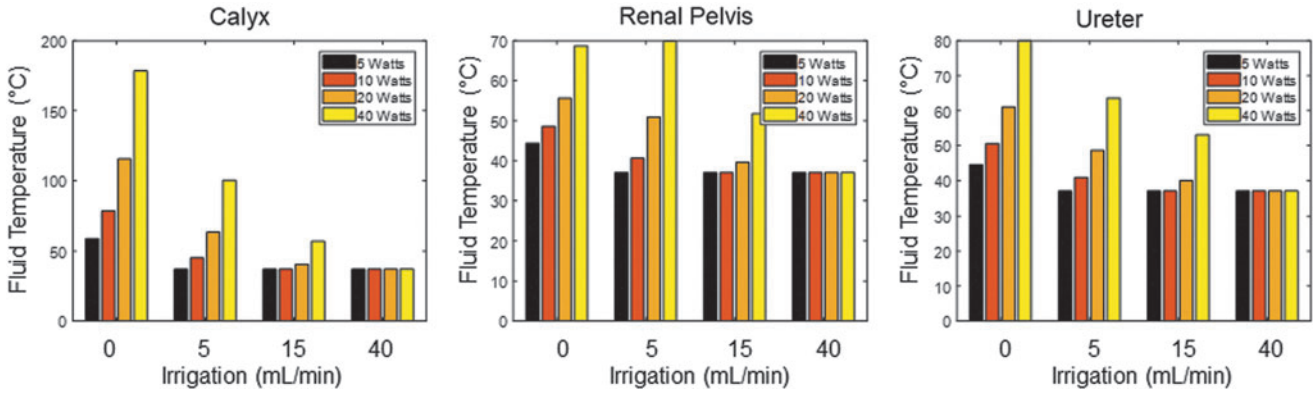

FIG. 4. *Bar plots* displaying volume-averaged temperature of urine reached within 60 seconds of laser pulsing under different parameters in a calyx (*left*), renal pelvis (*center*), and ureter (*right*).

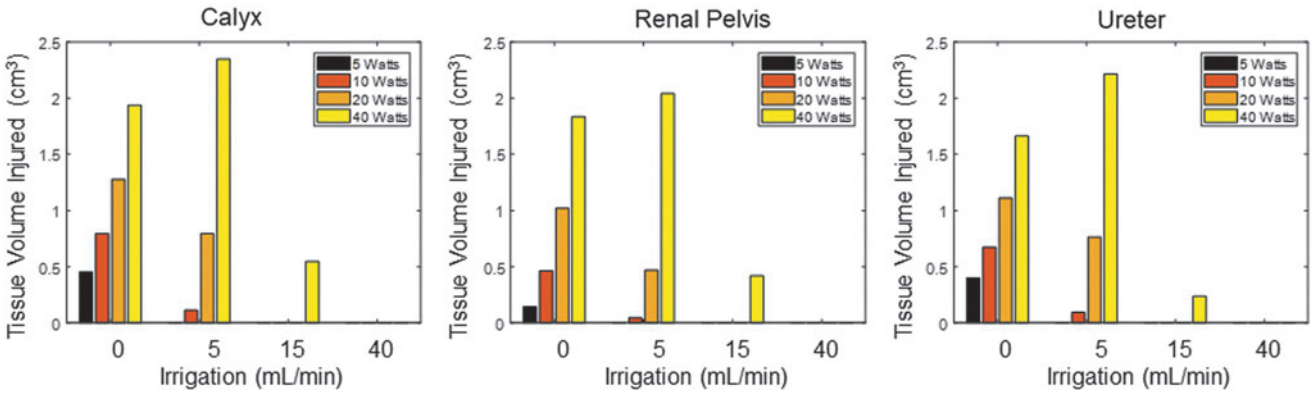

FIG. 5. Calculated volume of tissue injury (in cm^3) after simulation under different parameters in the calyx (*left*), renal pelvis (*center*), and ureter (*right*). No bar is shown for situations where volume was $<1\,mm^3$.

simulations with irrigation produced almost immediate tissue injury because of a localized jet of hot fluid carried to the surface.

Discussion

Holmium laser lithotripsy is the dominant instrumentation for disintegrating stones during URS. It is powerful enough to fracture nearly any stone type and the parameters allow control between fragmentation and dusting. Dusting is associated with shorter treatment times and fewer risks to the ureter,[17] and often uses more rapid pulsing and higher laser power, although trends in parameters vary between practices and across different parts of the world.[18] With introduction of new lasers using higher powers,[19] the potential for new bioeffects exists. The range of parameters modeled in this study are consistent with those used in commercial instruments.[19,20]

Light at the wavelength of a holmium laser is absorbed over a very short distance.[21] As a result, the water directly in front of the tip is boiled, producing a vaporous cavity between the fiber and stone. The remaining light energy of the pulse reaches the stone and causes disintegration through a photothermal effect.[21] After the pulse, the vapor cloud condenses back into liquid. Thus, the energy from the laser is transformed into two effects: creation of new surfaces in the stone and heating. The estimated mechanical energy expended to turn a stone into fragments is small. For instance, a 1 cm diameter sphere of gypsum cement (a common stone model) turned into 1 mm fragments would increase the surface area by a factor of $\sim$10, necessitating $\sim$50–100 mJ of energy. This is less than the typical energy of one pulse. Therefore, it can be assumed most of the energy is converted to heat. In this study, the total energy deposition ranged from 300 to 2400 J over 60 seconds. This energy is sufficient to heat an entire 150 cm^3 adult kidney by roughly 0.5–3.8°C. These estimates indicate that laser lithotripsy has the potential to cause a substantial temperature rise within a small volume.

This study demonstrates that laser lithotripsy heating can be numerically modeled. *In vitro*, both point and average fluid temperature in simulation agreed well with temperatures recorded in experiment with irrigation. However, simulated temperatures displayed larger discrepancies with measured data in the absence of irrigation. These data suggest absence of fluid mixing in the simulation as the likely reason. In practice, the growth and collapse of the boiling bubble stirs the fluid, likely producing dispersion of heat and more uniform temperature throughout the liquid.

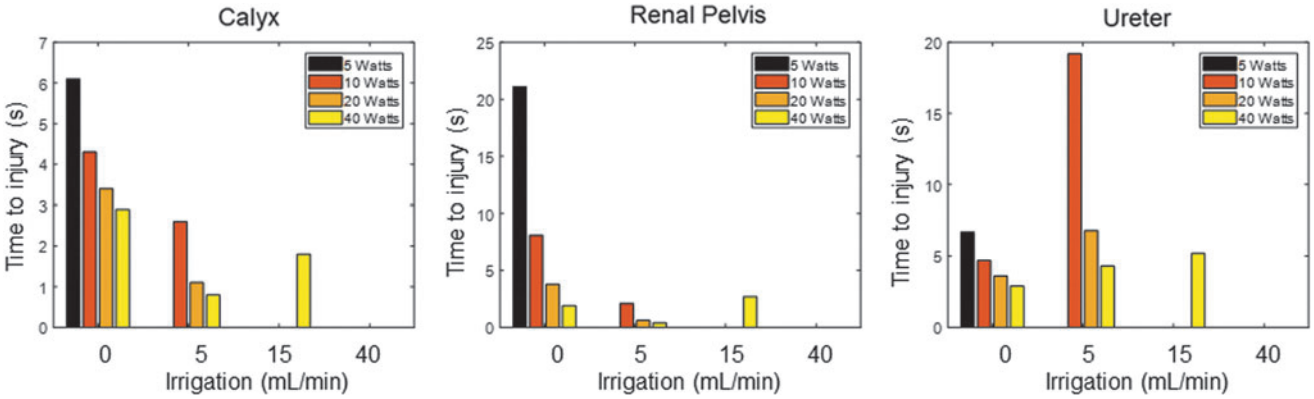

FIG. 6. Time to initiate injury (threshold $1\,mm^3$) under different pulsing and irrigation in the calyx (*left*), renal pelvis (*center*), and ureter (*right*). No bar is shown for situations where injury did not occur.

In simulated tissue, further complexity of heating was revealed. Without irrigation, even 5 W laser power deposited for <30 seconds could cause thermal injury. At maximum power in the calyx model without irrigation, injury to the wall and surrounding parenchyma was predicted over a 2 cm length around the fiber tip. With 5 mL/min irrigation, the damage was extended to >5 cm of the collecting space wall, but with minimal parenchymal injury. Irrigation sometimes reduced time to initiate injury, as the fluid transported hot liquid to the tissue faster than natural convection. Kidney parenchyma is highly perfused compared with other tissues that produced some protective effect, evident as a short pause in the onset of thermal injury at the boundary. Blood perfusion was insufficient to stop heating entirely, and in the most severe scenarios injury to >1 cm^3 of parenchyma occurred ($\sim$0.5% of an adult's functional renal volume[22]).

Although these results highlight the strong possibility of thermal injury during laser lithotripsy, the limitations of the model prevent drawing quantitative conclusions, and further data *in vivo* are needed to confirm these effects. The axisymmetric model is computationally efficient, but does not capture the complex flow and heat distribution in actual anatomy. In addition, this study did not capture variations in dimensions of the urinary tract that can be substantial between patients. However, our axisymmetric model also compared favorably with recent *in vivo* temperature data.[11] In addition, the presence of a stone could alter local heating around the laser fiber, but certain modes such as ''pop-dusting'' primarily deposit energy into the fluid. Aldoukhi and colleagues found *in vitro* with slow motion analysis that only 17.5% of pulses struck fragments with 0.5 J $\times$ 80 Hz parameters mimicking pop-dusting.[23] The fluid physics should include boiling and condensation to simulate added fluid motion and improve accuracy. Under moderate irrigation, the model gave a good approximation of the temperature expected during laser lithotripsy. Such models may provide valuable information to help define guidelines for safe parameters during laser lithotripsy.

Conclusions

We established a numerical model of heat generated during laser lithotripsy, which suggested that laser heating can cause significant temperature rises in the collecting system fluid and surrounding tissue. The temperature rises varied substantially with laser parameters, irrigation, and duration of pulsing. Under severe conditions, both the urinary tract and kidney parenchyma could reach temperatures sufficient to cause irreversible thermal injury. These findings may be clinically relevant particularly in light of trends toward high-power laser usage for treating stones.

Acknowledgment

This study was supported in part by a grant from the National Institutes of Health through NIDDK K01 DK104854.

Author Disclosure Statement

Adam Maxwell has equity and consulting arrangements with SonoMotion, Inc. No other competing financial interests exist.

References

1. Oberlin DT, Flum AS, Bachrach L, Matulewicz RS, Flury SC. Contemporary surgical trends in the management of upper tract calculi. J Urol 2015;193:880–884.
2. Krambeck AE, Murat FJ, Gettman MT, Chow GK, Patterson DE, Segura JW. The evolution of ureteroscopy: A modern single-institution series. Mayo Clin Proc 2006;81:468–473.
3. Rassweiler JJ, Knoll T, Köhrmann KU, McAteer JA, Lingeman JE, Cleveland RO, Bailey MR, Chaussy C. Shock wave technology and application: An update. Eur Urol 2011;59:784–796.
4. Duryea AP, Roberts WW, Cain CA, Tamaddoni HA, Hall TL. Acoustic bubble removal to enhance SWL efficacy at high shock rate: An *In Vitro* Study. J Endourol 2014;28:90–95.
5. Neisius A, Smith NB, Sankin G, et al. Improving the lens design and performance of a contemporary electromagnetic shock wave lithotripter. Proc Natl Acad Sci U S A 2014;111:E1167–E1175.
6. Alexander B, Fishman AI, Grasso M. Ureteroscopy and laser lithotripsy: Technologic advancements. World J Urol 2015;33:247–256.
7. Aldoukhi AH, Ghani KR, Hall TL, Roberts WW. Thermal response to high-power holmium laser lithotripsy. J Endourol 2017;31:1308–1312.
8. Molina WR, Silva IN, Donalisio da Silva R, Gustafson D, Sehrt D, Kim FJ. Influence of saline on temperature profile of laser lithotripsy activation. J Endourol 2015;29:235–239.
9. Butticè S, Sener TE, Proietti S, Dragos L, Tefik T, Doizi S, Traxer O. Temperature Changes Inside the Kidney: What Happens During Holmium:Yttrium–Aluminium-Garnet Laser Usage? J Endourol 2016;30:574–579.
10. Wollin DA, Carlos EC, Tom WR, Simmons WN, Preminger GM, Lipkin ME. Effect of laser settings and irrigation rates on ureteral temperature during holmium laser lithotripsy, an in vitro model. J Endourol 2018;32:59–63.
11. Aldoukhi AH, Hall TL, Ghani KR, et al. Calyceal fluid temperature during high-power holmium laser lithotripsy in an *in vivo* porcine model. J Endourol 2018;32:724–729.
12. Zelenko N, Coll D, Rosenfeld AT, Smith RC. Normal ureter size on unenhanced helical CT. AJR Am J Roentgenol 2004;182:1039–1041.
13. Wadekar P, Pundge S, Gangane S. The impact of lower infundibular length and lower infundibular width on renal stone formation. Inter J Healthcare Biomed Res 2014;2:158.
14. Schaeffer AJ, Kurtz MP, Logvinenko T, McCartin MT, Prabhu SP, Nelson CP, Chow JS. MRI-based reference range for the renal pelvis anterior–posterior diameter in children ages 0–19 years. Br J Rad 2016;89:20160211.
15. Sapareto SA, Dewey WC. Thermal dose determination in cancer therapy. Int J Radiat Oncol Biol Phys 1984;10:787–800.
16. Damianou C, Hynynen K. The effect of various physical parameters on the size and shape of necrosed tissue volume during cultrasound surgery. J Acoust Soc Am 1994;95:1641–1649.
17. Matlaga BR, Chew B, Eisner B, et al. Ureteroscopic laser lithotripsy: A review of dusting vs fragmentation with extraction. J Endourol 2018;32:1–6.
18. Aldoukhi AH, Roberts WW, Hall TL, Ghani KR. Holmium laser lithotripsy in the new stone age: Dust or bust? Front Surg 2017;4:57.

19. Elhilali MM, Badaan S, Ibrahim A, Andonian S. Use of the moses technology to improve holmium laser lithotripsy outcomes: A Preclinical Study. J Endourol 2017;31:598–604.
20. Hecht SL, Wolf JS. Techniques for holmium laser lithotripsy of intrarenal calculi. Urology 2013;81:442–445.
21. Chan KF, Pfefer TJ, Teichman JM, Welch AJ. A perspective on laser lithotripsy: The fragmentation processes. J Endourol 2001;15:257–273.
22. Johnson S, Rishi R, Andone A, et al. Determinants and functional significance of renal parenchymal volume in adults. Clin J Am Soc Nephrol 2011;6:70–76.
23. Aldoukhi AH, Roberts WW, Hall TL, Teichman JMH, Ghani KR. Understanding the popcorn effect during holmium laser lithotripsy for dusting. Urology 2018;122:52–57.

Address correspondence to:
Adam D. Maxwell, PhD
Department of Urology
University of Washington School of Medicine
1959 NE Pacific Street
Seattle, WA 98195

E-mail: amax38@u.washington.edu

Abbreviations Used
SWL = shockwave lithotripsy
URS = ureteroscopy